Developments in the Built Environment 23 (2025) 100693

Contents lists available at ScienceDirect

Developments in the Built Environment

journal homepage: www.sciencedirect.com/journal/developments-in-the-built-environment

Recovering hydrated cement from recycled concrete for improving technological properties of engineering bricks

P. Muñoz [a,b], V. Letelier [c,*], M. Bustamante [c], Osman Gencel [d], Milica V. Vasic [e]

[a] Escuela Superior de Ingeniería y Tecnología, Universidad Internacional de La Rioja, Avda. de la Paz, 137, Logroño, Spain
[b] Facultad de Ingeniería, Universidad Autónoma de Chile, 5 Poniente 1760, Talca, Chile
[c] Departamento de Obras Civiles, Universidad de la Frontera, Francisco Salazar 1145, Temuco, Chile
[d] Civil Engineering Department, Faculty of Engineering, Architecture and Design, Bartin University, 74100, Bartin, Türkiye
[e] Institute for Testing of Materials IMS, Bulevar vojvode Mišića 43, 11000, Belgrade, Serbia

ARTICLE INFO

Keywords:
Hydrated cement
Fired brick
Concrete recycling
Sustainability

ABSTRACT

In Europe, around 500 million tons of construction and demolition waste (C&DW) are generated annually, a third of which is concrete. Recycling mainly focuses on coarse aggregates, but 20–30 % v/v of the output includes fine particles and hydrated cement powder (HCP). As HCP can be partially reactivated at 450–650 °C, its reuse in clinker production is under study, though high energy demands hinder its viability. This research investigates an alternative: substituting clay with up to 30 % HCP in fired clay bricks, leveraging the high-temperature process already involved. Bricks were fired at three temperatures and characterised in terms of mechanical, mineralogical, chemical, and thermal behaviour. A life cycle impact assessment evaluated environmental feasibility. Results show that HCP enhances brick properties, especially at higher firing temperatures. However, despite improvements such as reduced thermal conductivity, global warming potential and water consumption impacts are higher, posing a trade-off between material performance and environmental cost.

1. Introduction

Construction and building industries act crucial for environmental conservation. Regardless the operation stage of buildings, the initial phase of construction materials (i.e. collection of raw materials, manufacturing and on site construction) certainly implies a large ecological footprint. Besides, the end life of buildings produces huge contents of construction and demolition waste (C&DW) (Ghisellini et al., 2018). As estimated, this residue stream represents about 30–40 % of total solid waste produced and its management market size reached $115 billion in 2020, worldwide. Although compound of C&DW changes from region to region, the main materials of these wastes come from concrete and ceramics, which represent between 70 % and 80 % (Wu et al., 2019; Bernardo et al., 2016).

For latest decades, concrete waste has been used to manufacture recycled aggregates (Silva et al., 2014). However, to be able to use these aggregates in cementitious materials it is necessary to apply different processes for cleaning adhered cement and fines particles e.g. conventional heating method, mechanical crushing method, acid leaching method, etc. (Wei et al., 2021). Due to its simplicity, one of the most used techniques is the removal or separation of hydrated cement powder (HCP) that coats natural aggregates from wear processes (Lu et al., 2018). Added to the recycled aggregates, these technologies also result in a large amount of fine powder residue (i.e. between 10 % and 20 %). The so produced waste powder contains large amounts of HCP which might be reused as alternative binder or supplementary cementitious material mainly for manufacturing more friendly concretes (Ma et al., 2022; Ohemeng, 2023).

However, because of its porous structure and high water absorption, this fraction has been commonly discarded or eventually used as an inert filler (Mehdizade et al., 2021; Xiao et al., 2018).

For instance, authors have demonstrated that with the increase of HCP content, the compressive strength and flexural strength of mortar at different ages decreased (Chen et al., 2021). In addition, during last decade research efforts have studied the thermal activation of waste cement (Real et al., 2020). Thus, several papers show the reactivity of this residue by proposing different preparation technologies to improve its performance (Bogas et al., 2022; Carriço et al., 2020). Besides, based on relative lower temperatures, the recovery of HCP may be a more sustainable process (Tokareva et al., 2023a). For instance, when

* Corresponding author. Departamento de Obras Civiles, Universidad de La Frontera, Francisco Salazar 1145, Temuco, Chile.
E-mail address: viviana.letelier@ufrontera.cl (V. Letelier).

https://doi.org/10.1016/j.dibe.2025.100693
Received 21 March 2025; Received in revised form 16 June 2025; Accepted 18 June 2025
Available online 19 June 2025
2666-1659/

compared to the ordinary cement manufacturing, some recovery strategies may reduce more than 50 % of the required thermal energy and more than 60 % of carbon emissions (Carriço et al., 2021; Sousa and Bogas, 2021).

Unfortunately, despite several experience which vary temperature (i.e. ranging from 450 °C to 1400 °C), particle size distributions or source of hydrated cement almost all research agree that compressive strength of recycled cement is still lower than compressive strength of ordinary cement (Wang et al., 2018).

For instance, although finer HCP particles might enhance compressive strength due to improved packing and pozzolanic activity (e.g. particle size from 50 μm to 10 μm), in most cases HCP content leads to strength loss (e.g. concrete strength dropped from 45.0 MPa to 35.9 MPa when HCP content rose from 0 % to 50 %) due to the relatively low hydraulic activity of HCP (Du et al., 2023).

Despite HCP has been extensively and deeply investigated in concrete manufacturing (Zhong et al., 2022) regarding the utilization in fired bricks, the available studies are so scarced. However, because of high temperatures needed in ceramic industry and the lower requirements in terms of mechanical strength, the replacement of clay by HCP might be a feasible way. To the best our knowledge, only two studies have previously studied the effect of powder from recycling concrete or a mixture of demolition residues (i.e. ceramic, mortar and concrete) in fired bricks (Bai et al., 2023; Osman et al., 2020).

However, two significant differences must be highlighted to justify the novelty of the present study. First, in the work of Gencel et al. (2020) (Osman et al., 2020), conducted at laboratory scale, the powder was produced directly through crushing concrete (CC) in a ball mill. As it did not undergo any secondary processing, its particle size was generally greater than 75 μm, which limited its reactivity and made it more suitable as a filler material rather than as a supplementary cementitious material. Second, in the studies by Bai et al. (2023) (Bai et al., 2023), the powder used consisted of demolition waste that included not only hydrated cement paste, but also brick, porcelain, and other debris (RP).

Thus, this paper explores the use of the replacement of only the selected finest fraction of HCP from the recycling of waste concrete aggregates as substitution for clay. In such a way that it dehydrates and regains its cementitious properties. Thus, the main hypothesis is that HCP may provide satisfactory technological properties to the so produced fired bricks helping to both reduce the use of clay and create a novel pathway for HCP reusing.

Besides, although according to Xiao et al. (2021) (Xiao et al., 2021), the future trend of the fired brick industry involves maximizing the utilization of construction waste, among others, a life cycle assessment (LCA) must be conducted for determining the environmental impact linked to the use of HCP. Therefore, this study also analyses the environmental impact of the fired bricks made with HCP.

2. Methods and materials

2.1. Samples manufacturing

Clay was collected from the quarry placed in Cauquenes, Chile. The location is commonly exploited for manufacturing refractory clays due to the high Al_2O_3 content (i.e. between 25 and 30 %) (Pardo et al., 2018). The powder has been obtained from an experimental plant which is fed with recovered aggregates from crushing plants (Fig. 1). This equipment comprises a sloping base where is placed a steel cylinder whose interior has a spiral profile. The cylinder rotates and the aggregates bounce off and bump into each other. Due to this process, hydrated cement and fines particles (HCP) come off from aggregates and the powder is collected through a grid (Fig. 1).

Clay and HCP were kept at 105 °C during 24 h and mixed in 10 kg batches. Several dosages were performed by replacing clay from 0 to 30 %. As shown in Table 1, amount of water was increased by increasing the replacement percentage. Despite it would be expected that the reduction of clay particles would lead to reduce water addition, the flocculation and agglomeration of clay grains in existence of CaO leads to reduce plastic index. The specific area of the soil is reduced as a result of the flocculation and cation exchange reactions that are quickly started by the lime addition. Due to this reason, content of water should be increased for obtaining enough working moisture (Mahan and Hussein, 2017).

Workability is a key factor for brick manufacturers since it influences extrusion and drying process, thereby final geometry and the risk of fissures or cracks in the fired bricks. Although the window for optimal extrusion is in between 15 % and 30 % (Bruno et al., 2019; Elavarasan et al., 2021), the addition of different residues or by-products certainly impacts on this range which may rise beyond 35 % (Zat et al., 2021; Muñoz et al., 2021). At low moisture, it is not possible to produce bricks without surface defects. Conversely higher water content resulted in a heterogeneous flux that also generated cracks and broken surface on bricks. Besides, the water content at the extrusion stage has great impact on fired bricks properties. Higher water content during the extrusion leads to increase porosity and therefore hinders compressive strength. In particular in this research a larger amount of water was necessary to

Fig. 1. Crushing machine used for collection HCP from demolished concrete wastes.

Table 1
Codes and dosages for each series.

ID.	Firing Temp. [°C]	Nº samples	Clay [%][a]	HCP [%][a]	Water [%][a]
A100HCP00a	1100	20	100	0.0	24.06
A95HCP05a		20	95.0	5.0	27.55
A90HCP10a		20	90.0	10.0	29.12
A85HCP15a		20	85.0	15.0	30.85
A80HCP20a		20	80.0	20.0	32.85
A75HCP25a		20	75.0	25.0	34.30
A70HCP30a		20	70.0	30.0	35.64
A100HCP00b	1000	20	100	0.0	24.09
A95HCP05b		20	95.0	5.0	27.11
A90HCP10b		20	90.0	10.0	29.12
A85HCP15b		20	85.0	15.0	30.85
A80HCP20b		20	80.0	20.0	32.05
A75HCP25b		20	75.0	25.0	33.86
A70HCP30b		20	70.0	30.0	35.64
A100HCP00c	900	20	100	0.0	24.26
A95HCP05c		20	95.0	5.0	26.15
A90HCP10c		20	90.0	10.0	28.01
A85HCP15c		20	85.0	15.0	31.11
A80HCP20c		20	80.0	20.0	32.05
A75HCP25c		20	75.0	25.0	33.86
A70HCP30c		20	70.0	30.0	35.55

[a] Percentages are expressed in dry basis of mixed blend.

form an extrudable blend due to the effect of HCP which compete with clay and reduces plasticity which leads to higher forming water.

In accordance with the followed industrial procedures, blends were formed by means of an extruder working at approx.10 MPa under vacuum conditions (Fig. 2).

Green specimens underwent through the drying process which was performed in an electrical furnace at 105 °C for 24 h. After that, dry specimens were fired by following the temperature curves showed in Fig. 3 at three different firing temperature of 900, 1000 and 1100 °C).

2.2. Characterization tests

Raw materials (i.e. clay and HCP) were characterized by means of different assays. Thus, particle size distribution (PSD) was obtained via hydrometer method in accordance with ASTM D7928-21e1 which is based on Stokes' law. Liquid limit and plastic limit were clarified in accordance with Casagrande technique in accordance with ASTM D4318. Thermogravimetric analysis (TGA) and a differential scanning calorimeter (DSC) were done under nitrogen atmosphere (i.e. from 25 to 900 °C, increasing rate of 10 °C/min) (PerkinElmer®, STA 6000). Chemical composition was carried out from XRF analysis (PANalytical®, Zetium). Mineral composition of both raw materials and samples, was analyzed via X-ray diffraction (XRD) (i.e. CuKα1, wavelength of 1.5418740) in the range of 5–80° 2θ (45 kV, 40 mA) (PANalytical®, Empyrean). These XRD patterns were also evaluated via crystallography open database Crystalimpact® by considering Rietveld method (Zhou et al., 2018). Regarding technological behavior of specimens, along the aforementioned process samples were weighted for determining shrinkage. A weighing balance (of ±0.1 g) and a caliper (of ±0.01 mm) were used to take measurements in accordance with NCh169 and EN 772-16 standards, respectively. In accordance with ISO 22007-2, transient plane source method was also used to obtain thermal diffusivity (d_f) and thermal conductivity (λ). Specific heat capacity (c_p) was computed using these values (Muñoz et al., 2022). According to ASTM C 373-18, bulk density, water absorption and porosity were determined. Moreover, compressive strength and flexural strength were assessed, in accordance with EN 1015–11:2019 (Uniform load between 10 and 50 N/s, failure between 30 and 90 s). Scanning electron microscope (SEM) (Hitachi®, SU3500) was utilized to view morphology. It also included energy dispersive X-ray spectroscope (Bruker®, QUANTAX) that allowed for chemical analysis of various regions in the picture.

2.3. Environmental impact assessment

The ecological footprint assessment was conducted by means of the SimaPro® software in accordance with ISO 14040:2006 and ISO 14044:2006 standards. The objective was to compare the environmental impact of conventional fired clay bricks with that of newly formulated alternatives. The comparison was based on a functional unit of 1 kg of fired product, considering a cradle-to-gate scope. This includes raw material extraction, material losses (20 %), transportation and manufacturing processes (i.e. clay grinding, mixing, aging, extrusion, cutting, drying, and firing). Due to this attribution approach, environmental benefits of avoiding landfilling for HCP were not accounted, in accordance with previous LCA analysis related to construction and demolition waste (Tefa et al., 2025). The life cycle inventory was built using input-output flows established in previous studies (Koroneos and Dompros, 2007) and the results showed in this study (see Fig. 4). Thus, 1 ton of fired bricks requires 1.2 tons of clay, the specific amount of water taken from Table 1 and 584.5 kWh of primary energy: Firing stage is fueled by natural gas (46.5 m^3 per Ton of fired clay), diesel is used for heavy machinery (0.54 kg per Ton of fired clay), while electricity (14.4 kWh per Ton of fired clay) is consumed by conveyors and other equipment. It must be noted that for accounting the energy required for firing temperature a firing temperature of 900 °C has been selected.

The drying stage benefits from heat recovery from the tunnel kiln,

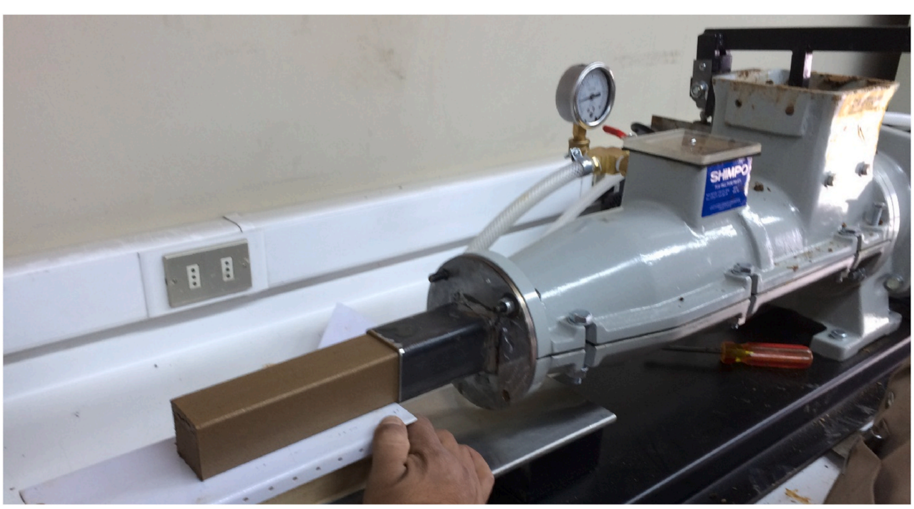

Fig. 2. Photography of the extrusion procedure.

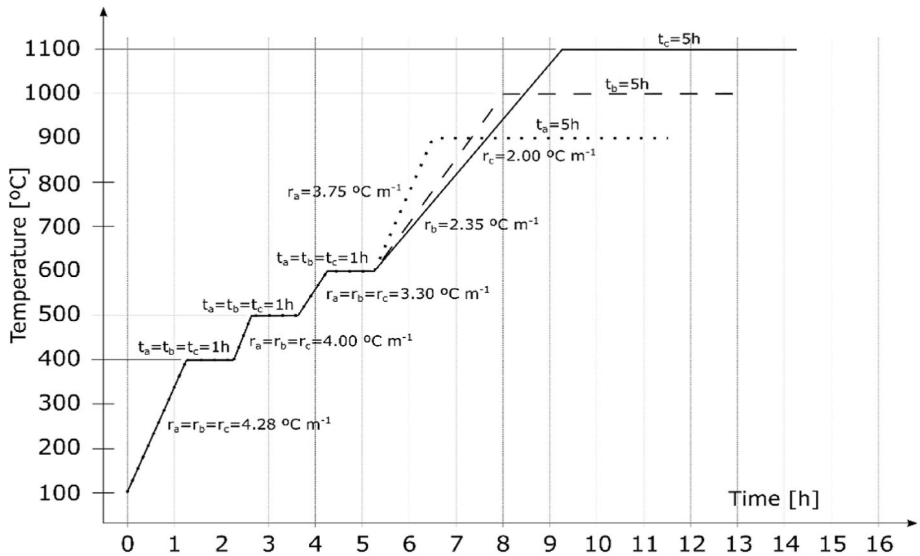

Fig. 3. Firing curves at each firing temperature.

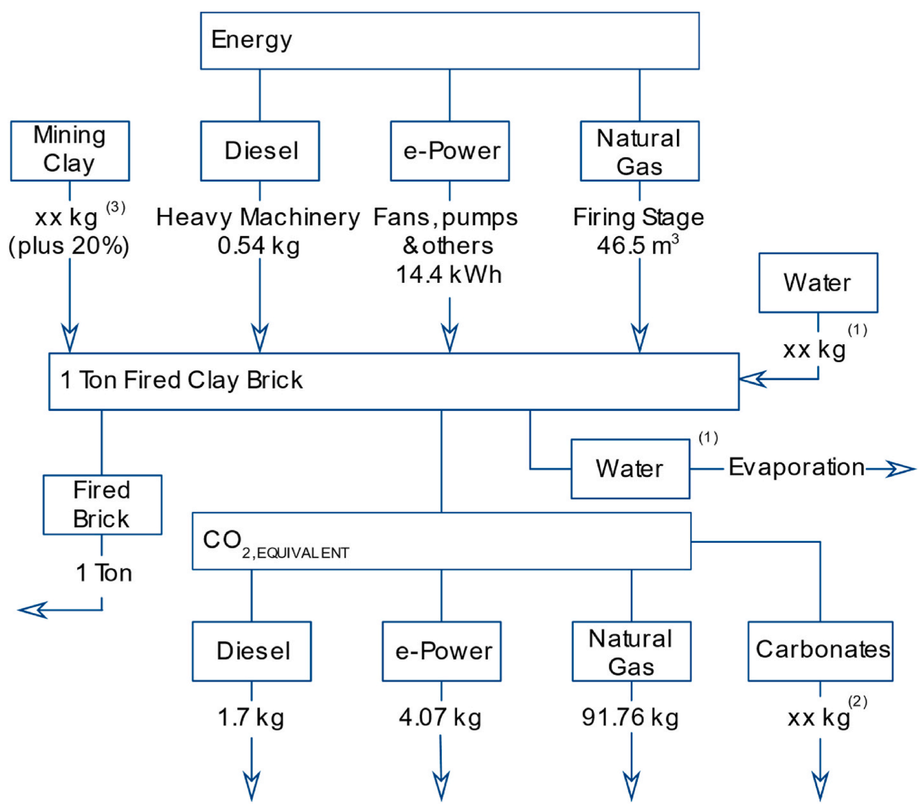

Fig. 4. LCA boundaries and input-output flows for 1 ton of fired clay bricks. (1) Water amount varies per Table 1 percentages; it's assumed all water used in molding evaporates during drying. (2) CO_2 emissions include natural gas combustion and decarbonation, calculated using TGA data based on the clay and HCP percentages in each mix. (3) The amount of raw clay varies in each mix from 1 Ton to 0.84 Ton.

thereby no extra heat is required (Kulkarni and Rao, 2016; Kaya and Mançuhan, 2009). In addition to GHG emissions from fuels combustion and electricity, CO_2 emissions from decarbonation were also considered, based on the obtained TGA curves (González et al., 2011). Related to the environmental impacts assessment, the Environmental Footprint 3.1 method was used by considering all 16 available indicators. Despite there is ongoing debate related to certain limitations about the applicability of this single scoring methodology (Martins Vaz et al., 2025), the European Commission certainly recommends it for normalisation and weighting criterion considering European data for average impacts. By integrating midpoint results into a single score, the method facilitates a holistic interpretation of environmental performance, making it particularly suitable for comparative analyses (Naumann et al., 2024).

3. Result and discussion

3.1. Results of raw materials

The used clay may be categorized as non-calcareous red clay due to low CaO amount and high percentage of iron oxides. Due to the low amount of carbonates, loss on ignition (approx. 6 %) shall be mainly produced by the organic content. This composition suggests that iron may be contained in the form of SFe and soluble sulphates ($FeSO_4$, $CaSO_4$, K_2SO_4, etc.) as it has been showed by previous studies which has been focused on clay deposits along this location (Pardo et al., 2018). Regarding mineral composition, XRD pattern (Fig. 5) suggests an illitic-kaolinitic nature of used clay as it has been demonstrated in previous investigations developed with same clay (Muñoz et al., 2020).

Like ash, HCP is commonly composed of high SiO_2 and AlO_3 contents (Tang et al., 2020). As it can be seen from oxides composition, SiO_2 and CaO are the most extended oxides (Table 2). While the HCP remains stocked, CO_2 and calcium bearing as well as unhydrated calcium silicates of HCP react to convert to calcium carbonate precipitation ($CaCO_3$) and calcium silicate hydrate (C-S-H) (Liu and Meng, 2021).

Fig. 5 presents high intensity of peaks related to calcite which is important phase showing carbonation of portlandite (i.e. Ettringite and C-S-H carbonation commonly led to aragonite and mix of calcite and vaterite, respectively) (Auroy et al., 2018). In addition, quartz and plagioclase feldspars (i.e. Andesine and Labradorite), from original concrete, are also showed which explain the presence of Na_2O (i.e. 6.47 %) and K_2O (1.37 %).

XRD pattern also shows Tobermorite or C-S-H that is one of the main hydrate components of concrete. As it has been stated, CO_2 reacts with cement and the hydration products. Hence, Carbonation causes C-S-H to decalcify and finally change into silica gel, which is denser than C-S-H (Liu and Meng, 2021).

TGA also corroborates XRD patterns and FRX analysis. Fig. 6 shows the removal of adhered water from C-S-H at approx. 200 °C (Liu et al., 2022) and a step at approx. 110 °C which can be identified as the decomposition of C-H-S (Phung et al., 2019) while at 700 °C the

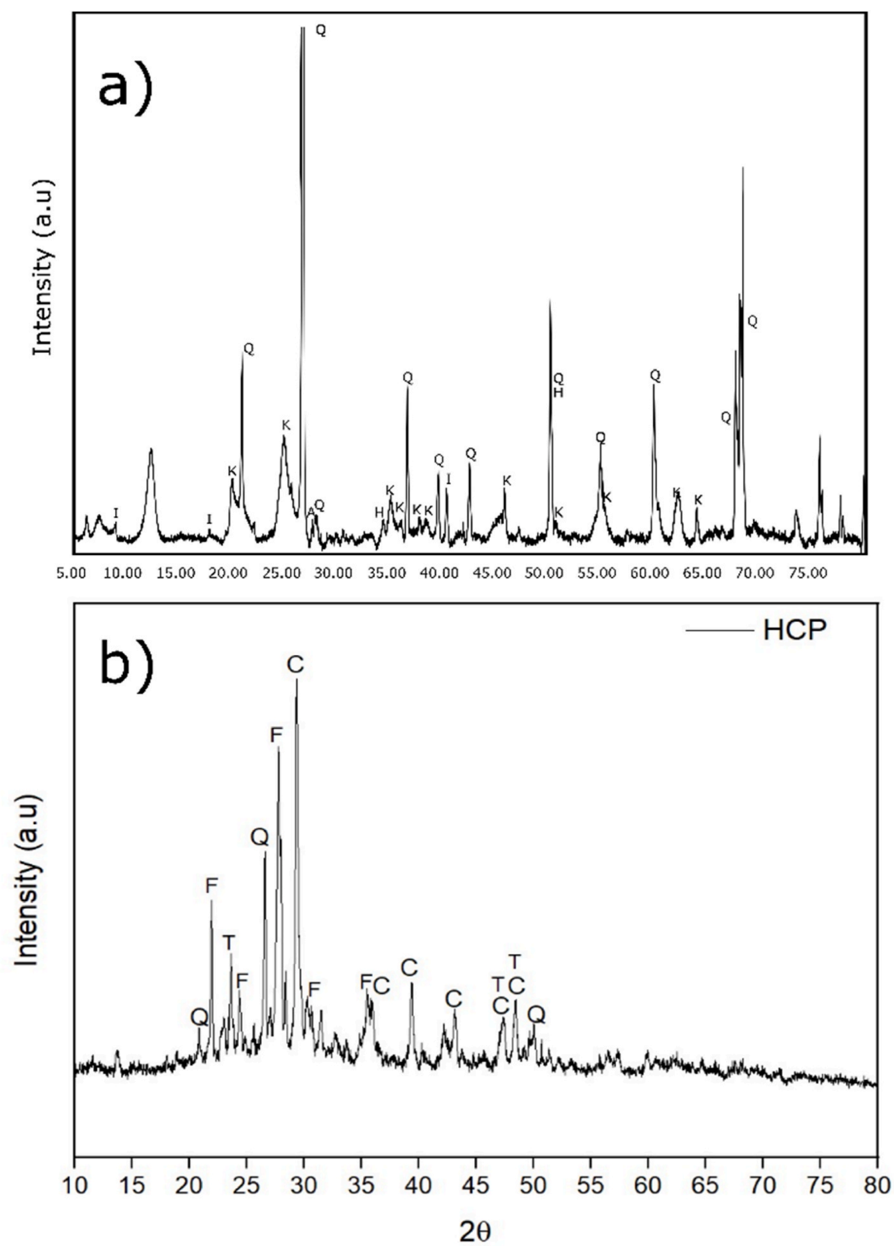

Fig. 5. XRD pattern of a) used clay (Muñoz et al., 2020) (b) HCP (Tobermorite (T); Calcite (C); Quartz (Q); Feldspars (F); Mica-Illite (I); Kaolinite (K).

Table 2
Oxide composition of clay and hydrated cement powder (HCP).

Element	SiO_2	Al_2O_3	Fe_2O_3	MnO	MgO	CaO	Na_2O	K_2O	TiO_2	P_2O_5	SO_3
Clay [%]	49.2	28.3	9.2	0.1	1.7	0.4	0.3	1.7	1.3	0.1	0.05
HCP [%]	30.7	10.5	6.3	–	1.6	39.2	6.5	1.4	0.6	–	3.33

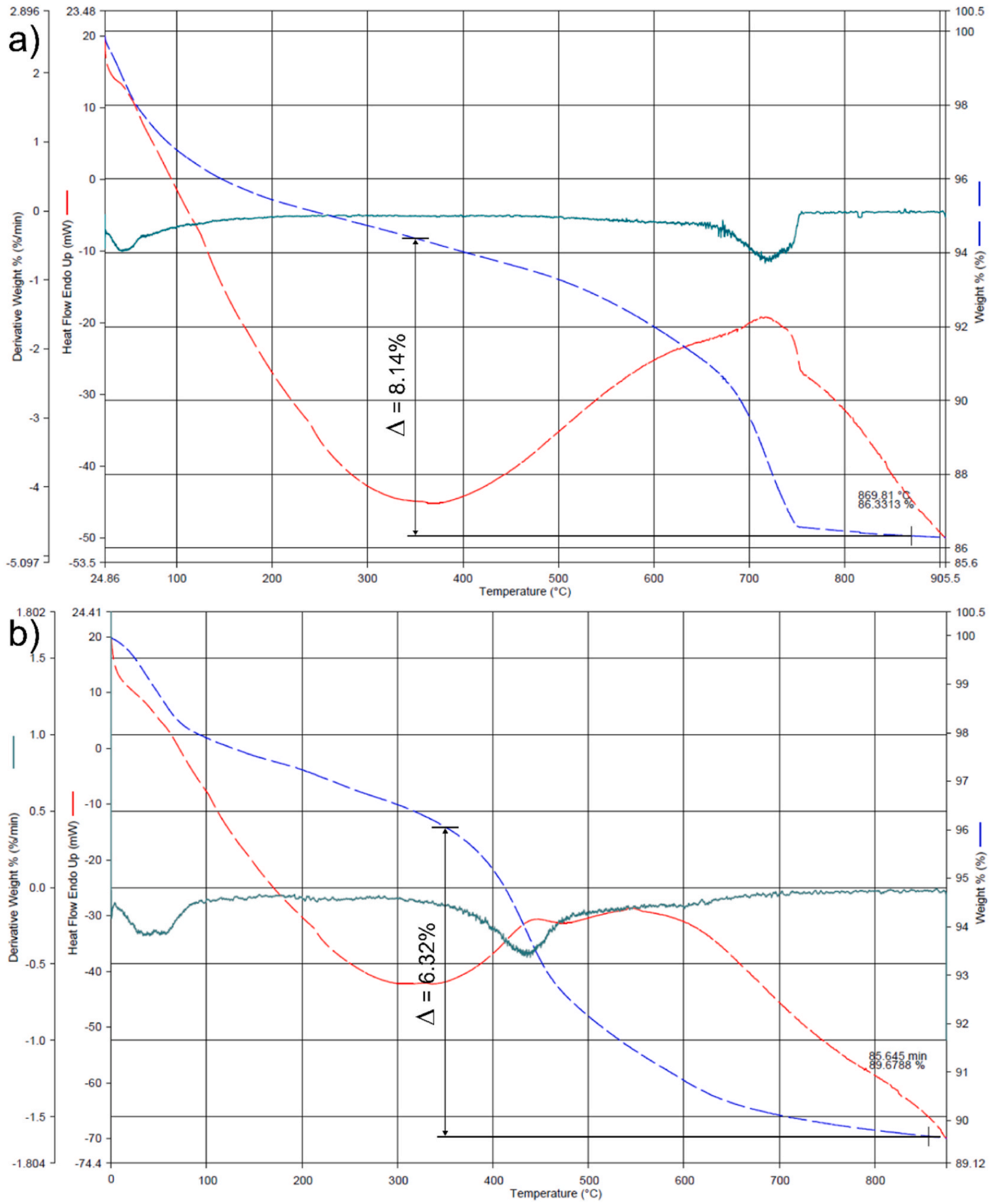

Fig. 6. TGA of a) HCP and b) clay.

reduction of weight is related to the calcite decarbonation. In the HCP, it is observed that no portlandite signals are present in the TGA (i.e., around 400 °C) (Klimesch and Ray, 1999). Although the crushed concrete originally contained cement, as it has been demostrated, the prolonged exposure of HCP to the weathering can lead to the dissolution of portlandite (Ayora et al., 1998). Related to the used raw clay, as it has been previously published, TGA first gives endothermic peak up to 100 °C because of moisture escape (Fig. 6b), and then via second smaller peak around 200 - 300 °C which can be related to the decomposition of goethite (FeOOH) into hematite (Wang et al., 2021). Endothermic peak shown (at 475 °C) that links with dehydroxylation of clay. Small exothermic peak indicates transition of α-quartz to ß-quartz (at 575 °C). At 600 °C, dehydroxylation of kaolinite and development of metakaolinite is seen (Faqir et al., 2019). Thermal decomposition at range of 500–970 °C are mainly related to limestone or carbonated materials content in sample which are the most important source for CO2 emissions (Rafael dos Santos et al., 2024).

Regarding the PSD of HCP, the largest percentage of particles corresponds to aggregates classification (i.e. more than 50 % above 20 um) while finest particles (i.e. below 2 um) represent less than 10 % (Fig. 7a). Therefore, in accordance with the Winkler diagram, the addition of HCP would reduce the overall percentage of clay particles but would not pose a barrier for manufacturing hollow or solid bricks (Fig. 7b) (Slížková et al., 2016).

3.2. Technological properties

Asit was expected, by increasing of firing temperature the mechanical performance increases in all cases. Besides, higher firing temperature also increases the effect of HCP replacement. Therefore, for samples fired at 900 °C the addition of HCP has little effect on compressive strength. However, when temperature rises, compressive strength shows a parabolic trend with a maximum at 5 %. From this percentage, compressive strength decays with a higher ratio as firing temperature raises.

In previous studies (Bai et al., 2023; Osman et al., 2020), strength also decreases with the incorporation of waste. Gencel et al. (Osman et al., 2020) fired the bricks at 1000 and 1100 °C and observed a reduction in strength from approx. 23.4 MPa–14.7 MPa for a 15 % of CC. Bai et al. (2023), at 900 °C reported a drop from 16.1 MPa to 9.0 MPa when 20 % of RP was added.

Effect of HCP can be related to both PSD and addition of CaO which both acts as binder and also as fluxing additive (Zaid et al., 2017). By adding HCP the amount of aggregates barely remains constant while clay content is reduced and fraction of silt grains increases. Therefore, fired matrix is rearranged as function of firing temperature and HCP addition which always leads to increasing the porosity and reducing compressive strength. In addition, as it has been previously stated, at low CaO amount, Ca^{2+} plays as gap-filling ion and repaired crystal defect so compressive strength is enhanced. Conversely, excess Ca^{2+} ions at high CaO content worked as network-modifier and fought for oxygen ions with silicon ions. As a result of this process, there are fewer bridging oxygens, which lowers the aggregates' crushing strength. (Liu et al., 2020). Same behavior can be observed from previous experiences with CaO rich wastes (Eliche-Quesada et al., 2017). Besides, both the role of water added for molding and the carbonates decomposition also play an important role. On the one hand, the thermal decomposition of carbonates increased porosity of fired clay bricks, with stress concentrations occurring as a result of the pore structure characteristics, leading to a reduction in the compressive strength of the brick specimens (Goel et al., 2021). On the other hand, the initial water-to-soil ratio highly impact on the porosity generated during the drying process. As it has been demonstrated, the higher amount of water due to both the HCP consumption and the necessary workability for extruding blends, leads to greater porosity, thereby effective resistant section is reduced (Zhao et al., 2022). Nevertheless, currently, fired bricks are mainly aimed to be part of the envelope rather than of the structure. From this point of view, the required mechanical resistance widely ranges by depending on the followed building code. Among the available standards, ASTM C62 classifies bricks as function of the weathering exposition and the

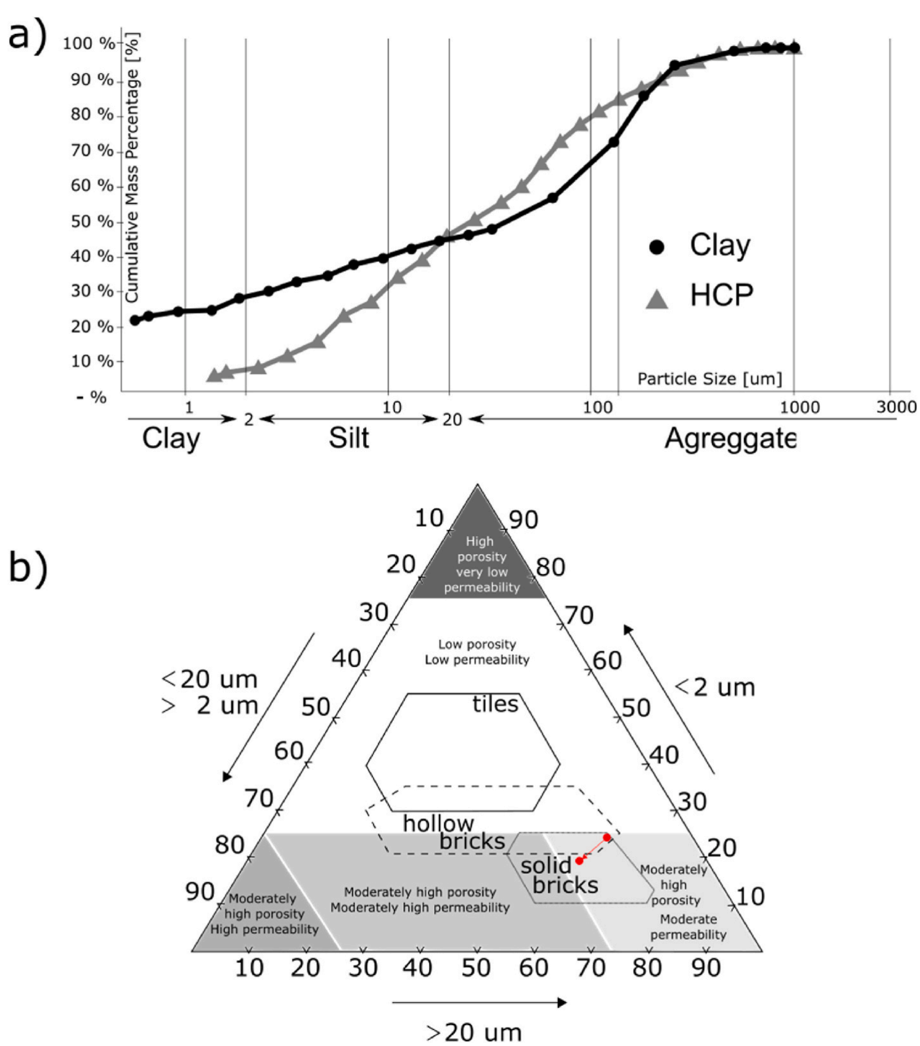

Fig. 7. a) PSD of clay and HCP and b) Location of original blend and admixtures within the Winkler's diagram.

compressive strength. Thus, for negligible (NW), moderate (MW) and severe weathering (SW) this standard states compressive strength benchmarks of 8.6, 15.2 and 17.2 MPa, respectively. The achieved compressive strength perspective leads to classify control samples fired at 900 °C and 1000 °C as grade NW, while specimens fired at 1100 °C can be considered comply with grade MW (Fig. 8a). Although flexural strength is not required by building codes, it certainly influences the mechanical response of walls, specially when horizontal loads are applied (Dominguez et al., 2017). The effect of adding HCP also leads to reduce flexural strength and the decay is more pronounced by increasing the firing temperature. Like compressive strength, flexural strength also tends to decrease as the calcareous content increases (Fig. 8b). Generally, flexural strength decreases exponentially as porosity increases but it does also depend on pore size and shape. For instance, flexural strength is positively impacted by spherically distributed, uniformly sized holes that range in size from 5 to 20 μm (Tavares-Brasileiro et al., 2021).

Water absorption is another significant parameter for brick manufacturers which has been widely recognized as one of the most reliable durability estimators (Abbas et al., 2017; Amira Sarani et al., 2023; Oubaha et al., 2023).

Through capillarity, water is absorbed to the fired clay matrix which might contribute to frost damage or salt crystallization (Franzoni et al., 2023). In particular, the dissolution and recrystallization of soluble salts within their porous systems highly affect the lifetime of the bricks (Crespo-López et al., 2024).

The crystallization of soluble salts (e.g. sulfates, chlorides or nitrates) in pores near the surface can generate internal pressures that can cause chipping or cracking, reducing the weathering resistance of the brick. However, none of the series produced have shown any signs of efflorescence that could pose a problem, at least in the short term (Fig. 9).

Thus, ASTM C62 classification not only requires for a minimum compressive strength but also for a maximum water absorption rate. From Fig. 10a, water absorption increased in all cases by increasing the HCP replacement ratio which is well aligned to the porosity behavior. Conversely, as it has been demonstrated, linear shrinkage (Fig. 11b) and absorption show inverse relationship (Ngun et al., 2011).

An increasing of carbonates led to formation of a porous body due to CO_2 release during firing stage (Martínez-Martínez et al., 2023). Thus, the carbonates formed during the ageing of HCP in the stockpile, are thermally decomposed and porosity is increased (Fig. 10b). Besides, by increasing HCP, free quartz is also increased. Since quartz expands more than clay minerals during the preheating stage porosity is further increased. In addition, the hydrophobic sand added by HCP presents opposite effect on moisture transportation and that results in weakening of capillary force among particles in clay matrix (Zhu et al., 2022). Considering impact of temperature, as it is usually exhibited, by increasing firing temperature more significant liquid phases are formed. These phases penetrate into pores, filling them and isolating from near pores (Semiz, 2017). However, by increasing temperature the slope of water absorption variation is also increased. Hence, for control series water absorption ranges from 18 % (i.e. fired at 900 °C) to 10.5 % (i.e. fired at 1100 °C) while for replacing 30 % difference is highly reduced (i.e. 21.8 to 20.2 %). At this point some authors suggest that large

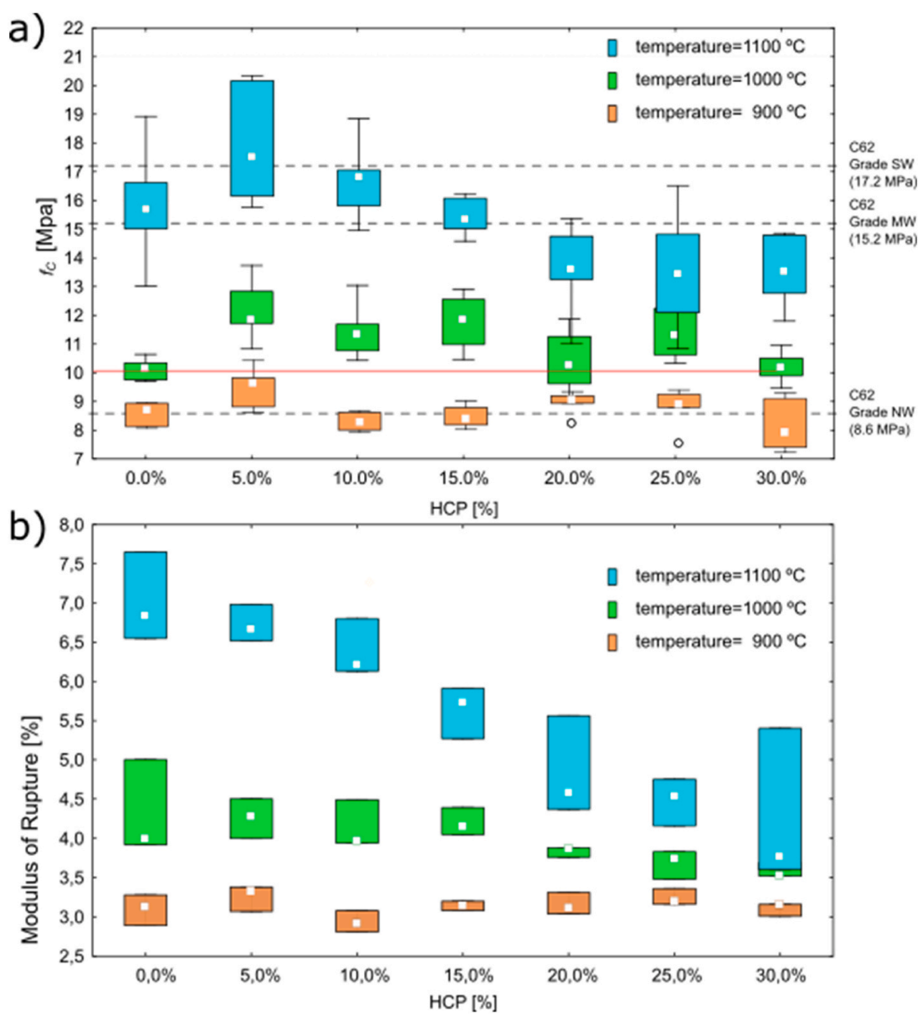

Fig. 8. a) Compressive strength and b) Modulus of rupture as function of firing temperature and HCP addition.

Fig. 9. Photography of fired samples. The legend in each sample corresponds to the identification showed in Table 1.

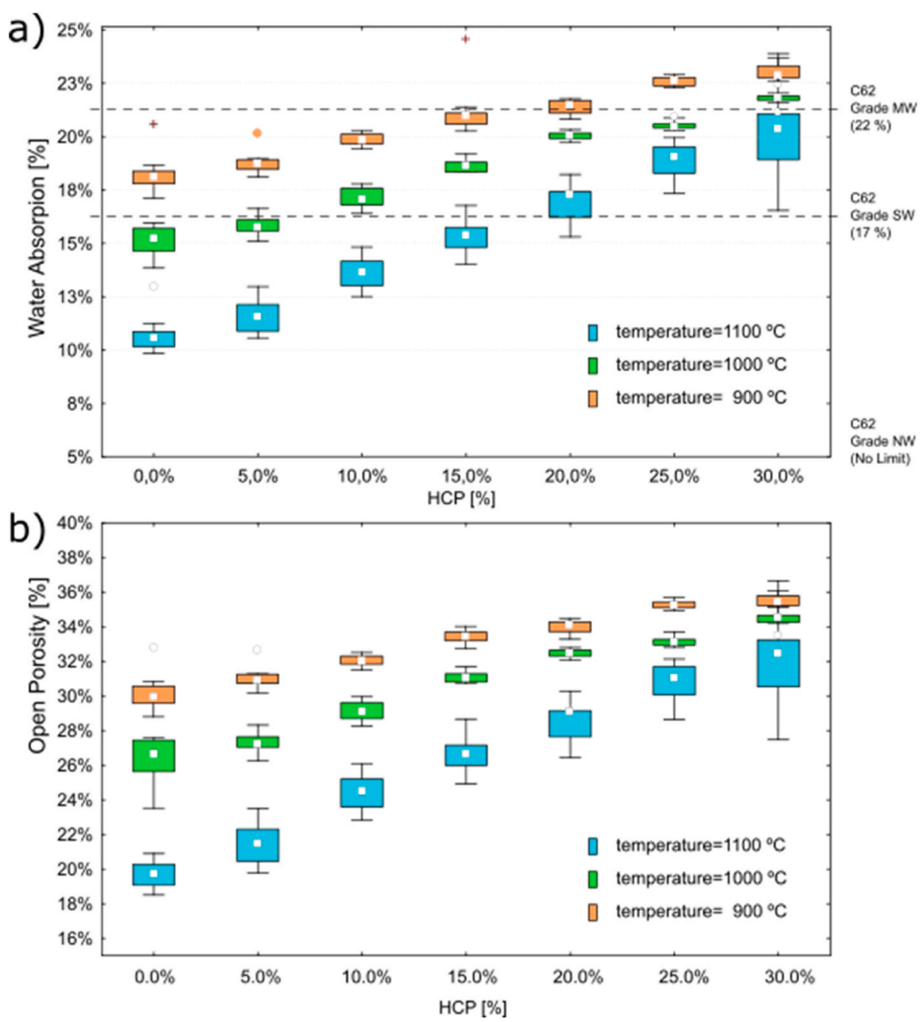

Fig. 10. Absorption and porosity as function of firing temperature and HCP addition.

percentage of Ca and Mg compounds result in minor descent of bulk density because of enlargement of entrapped gases (i.e. blisters and bloating) (Ke et al., 2013) (Fig. 11a). A similar decreasing trend is observed in related studies involving waste additions (e.g. between 8 % and 10 % for additions ranging from 15 % to 20 %) (Bai et al., 2023; Osman et al., 2020). Besides, the CaO reacts at the expense of amorphous phase (i.e. metakaolinite), that quickly disappears at the increased firing temperature (Baccour et al., 2009).

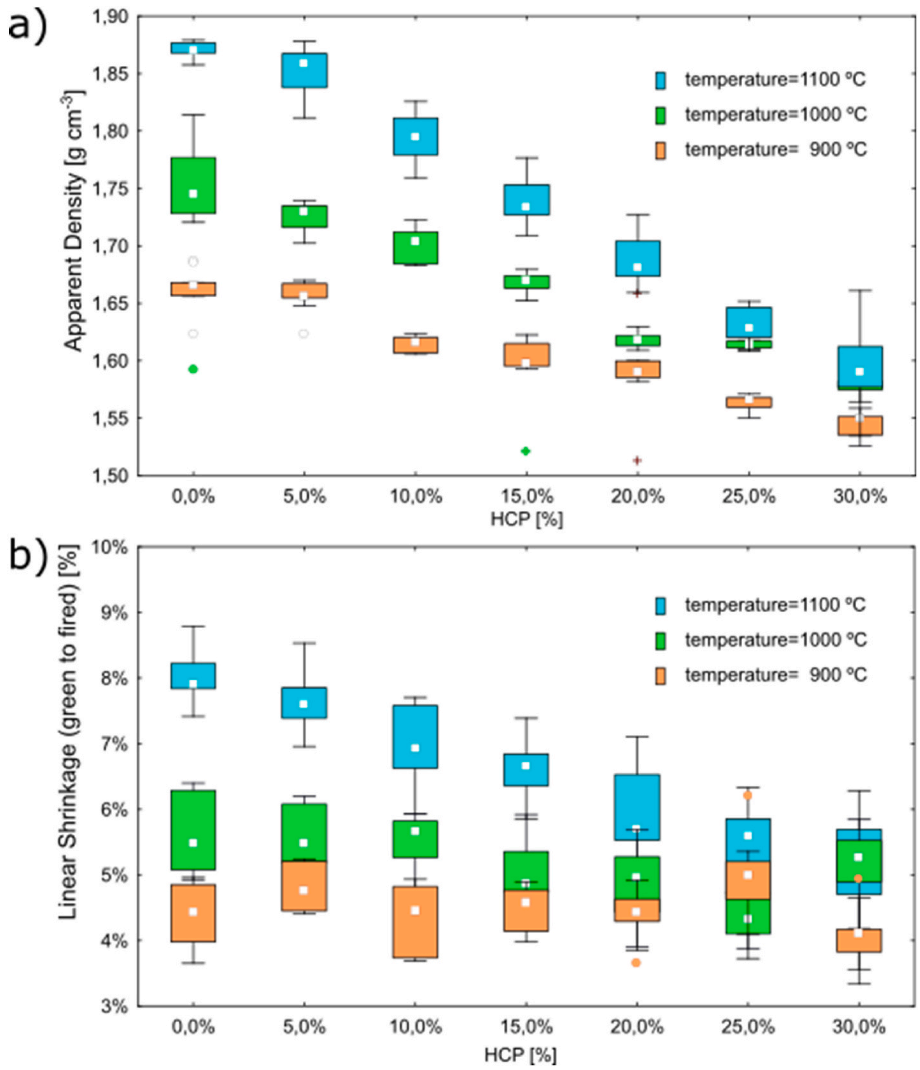

Fig. 11. Apparent density and total shrinkage as function of firing temperature and HCP addition.

Despite same has not been previously stated, as it has been aforementioned, some investigations may be compared. Thus, Gencel et al. (2020) (Osman et al., 2020) used concrete wastes for replacing up to 15 % of clay. Although similar trends were observed, the higher pressure during forming samples leads to minimize the effects of replacing ratio. For instance, at 15 % of replacement Gencel et al. (2020) (Osman et al., 2020) showed an increasing of water absorption of approx. 8 % at both 1000 °C and 1100 °C. However, in this paper, water absorption is increased 24 % and 46 % at 1000 °C and 1100 °C. Besides, same replacement percentage leads density to be reduced 5 % and 7 % for 1000 and 1100 °C in this research while related study showed only 3 % at both firing temperatures.

Fired bricks certainly must show a proper mechanical behavior, as it has been aforementioned. Nevertheless, nowadays they are mainly aimed for envelope so thermal behavior becomes even more importance than their mechanical strength. As commonly demonstrated, thermal conductivity is primarily related to porosity (Muñoz et al., 2016) (Fig. 12b). However, chemical composition of the fired matrix also influences its value. Wang et al. (2020) (Wang et al., 2020) determined that the increase of CaO in molten slags raises formation of non-bridging oxygen and decomposition of bridging oxygen. Therefore, instead of breaking down tetrahedral structure by creating a strong ionic Ca-O link, main mechanism for altering network structure of molten slag is association among two tetrahedral structures by O-Ca-O bonds. As result, phonon scattering is aggravated to decrease phonon mean free path, thus declining thermal conductivity. Similar by increasing NaO_2 content, amount of non-bridge oxygen also increases. This change causes frequency of phonon scattering higher which is explanation of low thermal conductivity in Na_2O-rich glasses (Hiroshima et al., 2008). Regarding the influence of firing temperature, as it has been showed, by lowering firing temperature thermal conductivity decreases (Nigay et al., 2017).

Besides, to develop better thermal behavior, heat capacity is also of great interest. Heat capacity together with thermal conductivity determine operating temperatures and temperature gradient which ultimately influences both thermal comfort and energy losses (Muñoz et al., 2022). Thus, specific heat capacity determines heat capacity of envelope and, thus, feasibility of heat storage. This behavior is of great importance when bioclimatic design aims to improve thermal comfort with the lowest energy consumption. Fig. 12a shows that the addition of HCP slightly increases the specific heat capacity. Conversely, it seems to be reduced by increasing firing temperature. According to the application of Neumann–Kopp's Law, heat content of mineral compound is total to sum of heat contents of its oxides. Despite for an equal oxides composition, different chemical bonds may lead to different heat capacities (Qiu and White, 2001), in case of silicate glasses, heat capacities are principally vibrational and can be clearly linked with ideal mixing of constant partial molar heat capacities of oxide components (Stebbins

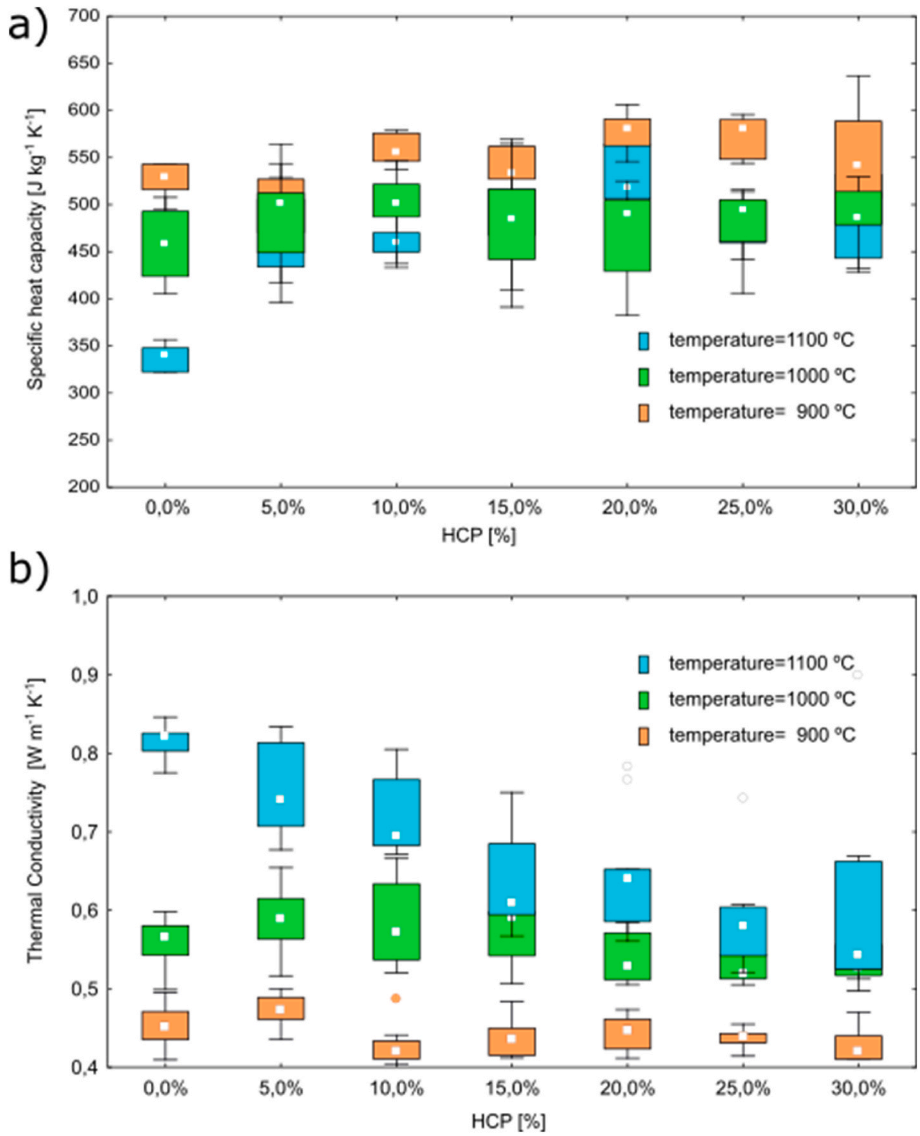

Fig. 12. Thermal characteristics as function of firing temperature and HCP addition.

et al., 1984). Thus, based on these statements, the slight increase specific heat capacity may be mainly attributed to the addition of Na_2O contained in HCP (Leitner et al., 2002).

Besides, specific heat temperature is reduced by increasing the firing temperature which is in accordance with previous authors that stated that thermal diffusivities increase with increasing temperature for CaO-Al_2O_3-SiO_2 ternary slag and its composition. The primary cause is attributed to the effects of cations on silicate network's structure and amphotheric behavior of alumina in the system (Eriksson and Seetharaman, 2004).

3.3. Mineral and microstructure assessment

From the XRD patterns (Fig. 13) it can be observed, regardless the firing temperature, that both Andesine and Albite peaks are increased when the percentage of HCP is increased while peaks related to quartz are reduced which is in agreement with previous authors (Cultrone and Carrillo Rosua, 2020). Besides, this effect would also explain the reduction of compressive strength, as it has been previously reported (Sadik et al., 2014). During the firing process, HCP is dehydrated and reacts with the clay minerals and quartz phases. The effect is more noticeable in XRD patterns of series fired at 1000 °C and 1100 °C. However, by increasing replacement ratio from 15 % the higher content of CaCO3 modifies the CaO:SiO2 ratio which greatly influences compressive strength due to the variation of melting temperatures (Tabit et al., 2020). As it has been showed (Fig. 8), these unbalanced CaO:SiO2 ratios and the increasing of porosity due to the decomposition of carbonates, mechanical strength is reduced. However, in contrast to previous studies (Yaras et al., 2019), the trend shows a more moderate decline which may be attributed to the presence of feldspar in HCP which act as fluxing agents (i.e. plagioclase) (Fuertes et al., 2022). This effect is also corroborated by SEM images (Fig. 14) which show that crystalline phases are developed at earlier stages for higher percentage of HCP addition. As result, these series show lower degree of vitrification but a more ordered pore distribution. In addition, SEM images show how the increasing of fluxing agents promotes larger fissures during the firing process, as it has been previously reported in similar studies (Loryuenyong et al., 2009; Tokareva et al., 2023b).

It has been demonstrated that uneven stress distribution at long grains leads to increased microscopic cracks and poor physical properties which is unfavorable to the mechanical property of fired bricks (Lim and Mondal, 2014). Similar studies has shown similar effect. For instance, Bai et al. (2023) showed the same pore enlargement with the increasing content of recycled powder (Bai et al., 2023). This effect

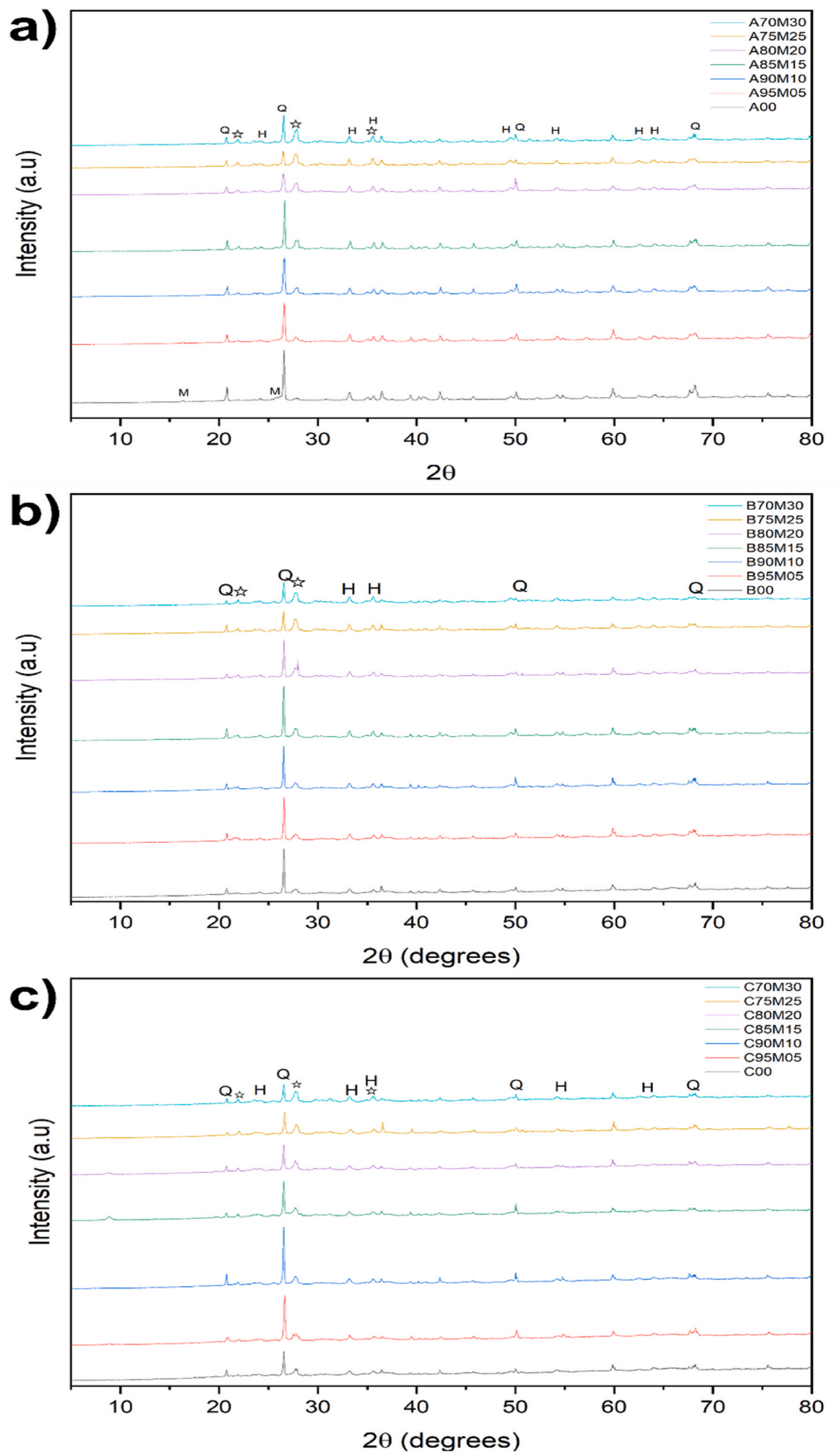

Fig. 13. XRD of samples fired at different temperatures and made with replacement ratios a) 900 °C, b) 1000 °C and c) 1100 °C. ☆: plagioclase (Andesine - Albite); Q: quartz; H: hematite; M: mullite.

might be explained by the cement paste fragmentation at the temperature around 900 °C (Georgali and Tsakiridis, 2005). However, although at higher temperatures, micro-cracks should become wider, metakaolin particles acts as fibers bridges the micro cracks in the matrix which provide resistance to crack propagation and crack opening (AL-Salami et al., 2013). Besides, the continuous rise of temperature eases the nucleation and growth of crystals. With the help of the liquid phase, crystals adhere to each other to form a stronger skeleton structure (Wang et al., 2023).

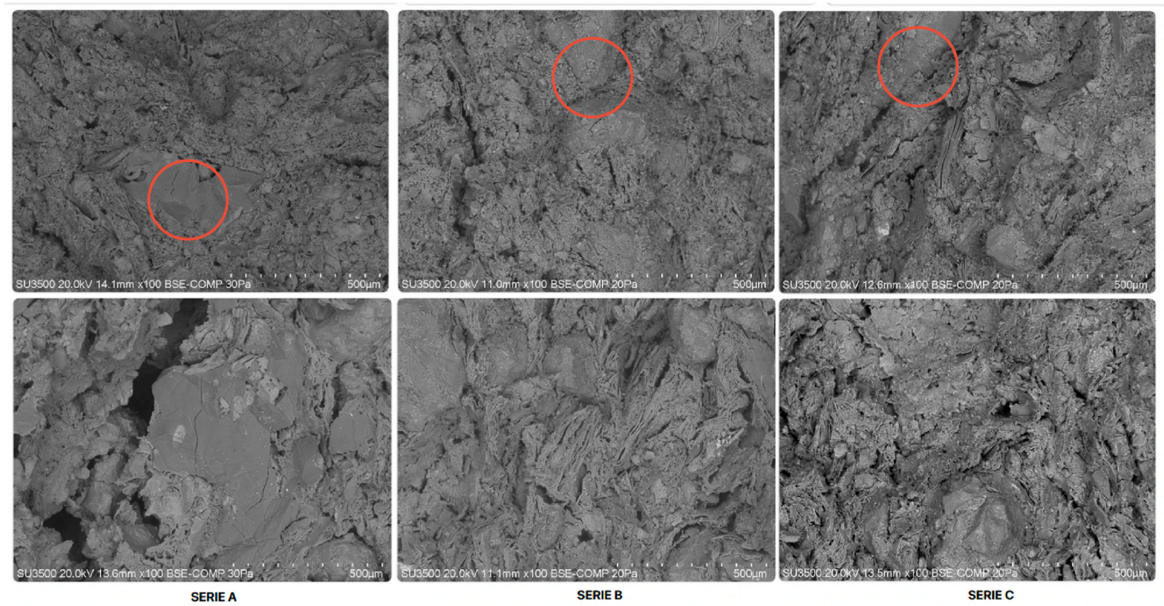

Fig. 14. SEM images for control samples fired at 900 °C (a), 1000 °C (b), 1100 °C (c) and A70PC30 series fired at 900 °C (d), 1000 °C (e), 1100 °C (f).

3.4. Environmental impacts

Related to the environmental impacts, a consistent increase in greenhouse gas emissions is observed with higher cement content (Fig. 15). The higher impacts are attributed to the higher amount of carbonates contained in HCP which are decomposed into oxides and CO_2 and may rise up to 10 % (Gonzá et al., 2011) or beyond (Warrier et al., 2024).

Although a slight increase is observed in the indicator associated with global warming potential (GWP), this impact should be considered in light of several mitigating factors. In particular, lime-based products are prone to carbonation throughout their service life, which involves the reabsorption of carbon dioxide. For instance, a carbonation rate of 90 % has been reported after 50 years of service (George et al., 2018). On the other hand, the increase in mechanical strength observed for additions up to 15 % could enable a reduction in firing temperature (within any of the applicable ranges), which would result in an improvement of these environmental indicators. Nevertheless, it is worth noting that the contribution associated with the handling of HCP has not been considered in the LCA, since this powder must, in any case, be managed as inert landfill waste. Therefore, depending on the exact location of the HCP stockpile and the brick manufacturing facility, the potential environmental impact of transport should be accounted (George et al., 2018).

In addition, impacts related to water consumption increase

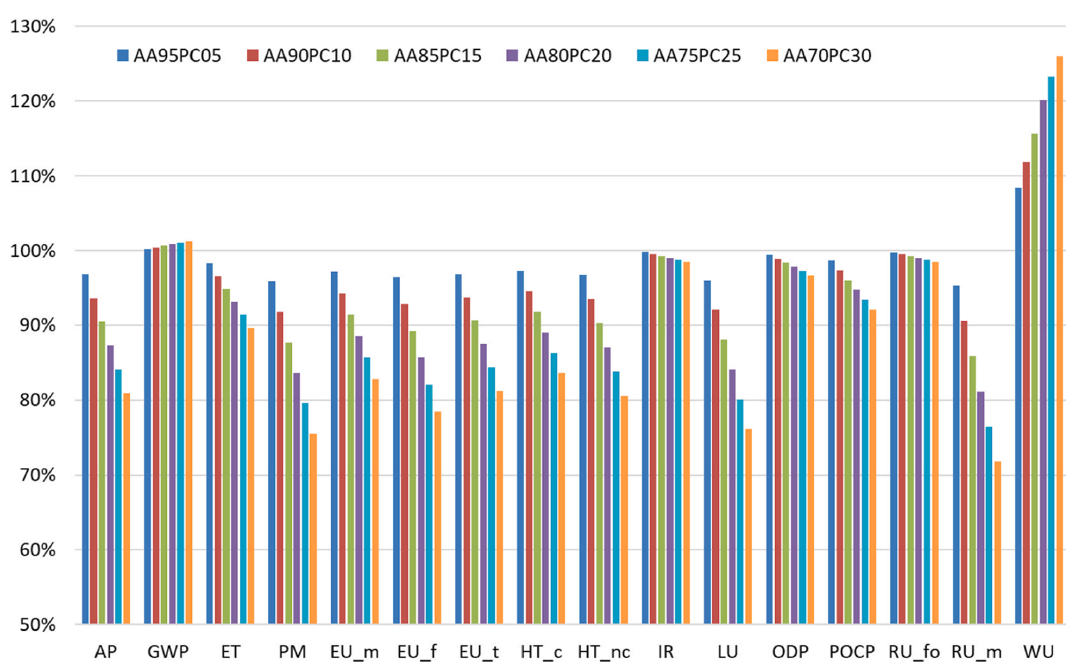

Fig. 15. Results of the impact assessment method: acidification potential (AP), ecotoxicity-freshwater (ET), energy resources-non-renewable (RU_fo), eutrophication-freshwater (EU_f), eutrophication-marine (EU_m), eutrophicationterrestrial (EU_t), global warming potential (GWP), human toxicity-carcinogenic (HT_c), human toxicity-non-carcinogenic (HT_nc), ionizing radiation (IR), land use (LU), material resources-metals/minerals (RU_m), ozone depletion potential (ODP), particulate matter formation (PM), photochemical oxidant creation potential (POCP), and water use (WU).

significantly as the HCP content rises, due to the greater amount of water required for extruding the admixtures. It should be noted that, in this study, the water used for shaping was applied in liquid form, in contrast to modern industrial practice, which typically employs steam or plasticisers to significantly reduce the amount of water needed to achieve the required workability of the clay body during extrusion (Morales et al., 2014). Moreover, the implementation of various water recovery strategies and the use of alternative water sources (other than potable water supply) can reduce water demand by up to 80 % [93].

Conversely, the rest of categories decrease progressively with higher HCP content due to the lower natural clay that must be collected from quarries and the associated environmental burdens. Thus, the control clay-based brick shows the lowest water consumption and global warming potential, but the highest values in toxicity, eutrophication, particulate matter, and ecotoxicity, underlining that pure clay is not necessarily the most environmentally favorable option overall. No single formulation excels in all environmental categories.

Additionally, it is worth highlighting that the reduction in the thermal conductivity of the newly developed bricks (along with the potential combined effects of their specific heat capacity values) could lead to energy savings in buildings where they are used. Although this aspect has not been directly addressed in the present study, it is well established that lowering thermal conductivity values can result in significant reductions in energy consumption, depending on the final geometry of the bricks and the construction systems employed [94].

4. Conclusion

The hydrated cement powder is produced during the recycling of concrete. Although it can be reactivated at high temperatures, the insufficient quality of the resulting product mostly causes to be discarded and merely disposed in landfills. However, this paper has demonstrated that brick industry may use it for replacing natural clay with positive effects. In general, the addition of this powder leads to lighter fired products with lower thermal conductivity and similar compressive strength. It has been showed that by increasing temperature the effect of the addition is increased. At 5 % the compressive strength is increased when comparing to control series for all firing temperatures. This percentage would be the most suitable replacement ratio in accordance with ASTM C62 requirements. Indeed, bricks with 5 % of addition and fired at 1100 °C can be used for structural purposes under severe weathering.

In addition, in future research more tests related to the bricks' long-term durability should be necessary for scaling this proposal (e.g. accelerated aging tests, freeze-thaw cycle evaluations or resistance to recristallization, among others).

CRediT authorship contribution statement

P. Muñoz: Writing – original draft, Formal analysis, Conceptualization. **V. Letelier:** Writing – original draft, Project administration, Conceptualization. **M. Bustamante:** Writing – original draft, Formal analysis. **Osman Gencel:** Writing – review & editing, Writing – original draft, Investigation. **Milica V. Vasic:** Writing – review & editing.

Declaration of competing interest

The authors declare that they have no known competing financial interests or personal relationships that could have appeared to influence the work reported in this paper.

Acknowledgements

The investigation is financed by the Chilean National Commission on Research and Development with grant number 1211135. Additionally, the authors gratefully acknowledge the partial support from Universidad de La Frontera (Chile) and Ministerio de Educación (MINEDUC) (Project FRO 2395).

Appendix A. Supplementary data

Supplementary data to this article can be found online at https://doi.org/10.1016/j.dibe.2025.100693.

Data availability

Data will be made available on request.

References

Abbas, Safeer, Saleem, Muhammad A., Kazmi, Syed M.S., Munir, Muhammad J., 2017. Production of sustainable clay bricks using waste fly ash: mechanical and durability properties. J. Build. Eng. 14, 7–14. https://doi.org/10.1016/j.jobe.2017.09.008.

Al-Salami, A.E., Morsy, M.S., Taha, S., Shoukry, H., 2013. Physico-mechanical characteristics of blended white cement pastes containing thermally activated ultrafine nano clays. Constr. Build. Mater. 47, 138–145. https://doi.org/10.1016/j.conbuildmat.2013.05.011.

Amira Sarani, Noor, Kadir, Aeslina Abdul, Din, Mohd Fadhil Md, Hashim, Azini Amiza, Hassan, Mohd Ikhmal Haqeem, Hamid, Nur Jannah Abdul, Hashar, Nurul Nabila Huda, Hissham, Nur Fatin Nabila, Johan, Siti Farhanah S.M., 2023. Physical-mechanical properties and thermogravimetric analysis of fired clay brick incorporating palm kernel shell for alternative raw materials. Constr. Build. Mater. 376, 131032. https://doi.org/10.1016/j.conbuildmat.2023.131032.

Auroy, M., Poyet, S., Le Bescop, P., Torrenti, J.-M., Charpentier, T., Moskura, M., Bourbon, X., 2018. Comparison between natural and accelerated carbonation (3% CO2): impact on mineralogy, microstructure, water retention and cracking. Cement Concr. Res. 109, 64–80. https://doi.org/10.1016/j.cemconres.2018.04.012.

Ayora, C., Chinchón, S., Aguado, A., Guirado, F., 1998. Weathering of iron sulfides and concrete alteration: thermodynamic model and observation in dams from central pyrenees, Spain. Cement Concr. Res. 28 (4), 591–603. https://doi.org/10.1016/S0008-8846(98)00019-2.

Baccour, H., Medhioub, M., Jamoussi, F., Mhiri, T., 2009. Influence of firing temperature on the ceramic properties of Triassic clays from Tunisia. J. Mater. Process. Technol. 209 (6), 2812–2817. https://doi.org/10.1016/j.jmatprotec.2008.06.055.

Bai, Meiyan, Xiao, Jianzhuang, Qi, Gao, Shen, Jianyu, 2023. Utilization of construction spoil and recycled powder in fired bricks. Case Stud. Constr. Mater. 18, e02024. https://doi.org/10.1016/j.cscm.2023.e02024.

Bernardo, M., Castilho Gomes, M., de Brito, J., 2016. Demolition waste generation for development of a regional management chain model. Waste Manag. 49, 156–169. https://doi.org/10.1016/j.wasman.2015.12.027.

Bogas, J.A., Real, S., Carriço, A., Abrantes, J.C.C., Guedes, M., 2022. Hydration and phase development of recycled cement. Cement Concr. Compos. 127, 104405. https://doi.org/10.1016/j.cemconcomp.2022.104405.

Bruno, Agostino Walter, Gallipoli, Domenico, Perlot, Céline, Mendes, Joao, 2019. Optimization of bricks production by earth hypercompaction prior to firing. J. Clean. Prod. 214, 475–482. https://doi.org/10.1016/j.jclepro.2018.12.302.

Carriço, A., Bogas, J.A., Guedes, M., 2020. Thermoactivated cementitious materials – a review. Constr. Build. Mater. 250, 118873. https://doi.org/10.1016/j.conbuildmat.2020.118873.

Carriço, A., Bogas, J.A., Hu, S., Real, S., Costa Pereira, M.F., 2021. Novel separation process for obtaining recycled cement and high-quality recycled sand from waste hardened concrete. J. Clean. Prod. 309, 127375. https://doi.org/10.1016/j.jclepro.2021.127375.

Chen, Xi, Li, Ying, Bai, Hualei, Ma, Liyuan, 2021. Utilization of recycled concrete powder in cement composite: strength, microstructure and hydration characteristics. J. Renewab. Mater. 9 (12). https://doi.org/10.32604/jrm.2021.015394.

Crespo-López, Laura, Coletti, Chiara, Arizzi, Anna, Cultrone, Giuseppe, 2024. Effects of using tea waste as an additive in the production of solid bricks in terms of their porosity, thermal conductivity, strength and durability. Sustain. Mater. Technol. 39, e00859. https://doi.org/10.1016/j.susmat.2024.e00859.

Cultrone, G., Carrillo Rosua, F.J., 2020. Growth of metastable phases during brick firing: mineralogical and microtextural changes induced by the composition of the raw material and the presence of additives. Appl. Clay Sci. 185, 105419. https://doi.org/10.1016/j.clay.2019.105419.

Dominguez, D., Muñoz, V.P., Muñoz, V.L., 2017. Impact of using lightweight eco-bricks as enclosures for individual houses of one story on zones of high seismicity. Mater. Construcción 67 (328), e133. https://doi.org/10.3989/mc.2017.03316.

Du, Junpeng, Zhang, Tongsheng, Chen, Peixin, Guo, Yiqun, Zhan, Binggen, Wei, Jiangxiong, Yu, Qijun, 2023. Phase separation of recycled concrete powder during grinding and consequent influences on its hydration behaviors in cement paste. Cement Concr. Compos. 142, 105203. https://doi.org/10.1016/j.cemconcomp.2023.105203.

Elavarasan, S., Priya, A.K., Kavin Kumar, V., 2021. Manufacturing fired clay brick using fly ash and M−Sand. Mater. Today Proc. 37 (Part 2), 872–876. https://doi.org/10.1016/j.matpr.2020.06.042.

Eliche-Quesada, D., Felipe-Sesé, M.A., López-Pérez, J.A., Infantes-Molina, A., 2017. Characterization and evaluation of rice husk ash and wood ash in sustainable clay matrix bricks. Ceram. Int. 43 (1), 463–475. https://doi.org/10.1016/j.ceramint.2016.09.181.

Eriksson, R., Seetharaman, S., 2004. Thermal diffusivity measurements of some synthetic CaO-Al2O3-SiO2 slags. Metall. Mater. Trans. B 35 (3), 461–469. https://doi.org/10.1007/s11663-004-0047-z.

Faqir, N.M., Shawabkeh, R., Al-Harthi, M., et al., 2019. Fabrication of geopolymers from untreated kaolin clay for construction purposes. Geotech. Geol. Eng. 37, 129–137. https://doi.org/10.1007/s10706-018-0597-5.

Franzoni, Elisa, Berk, Bensu, Bassi, Mattia, Marrone, Clelia, 2023. An integrated approach to the monitoring of rising damp in historic brick masonry. Constr. Build. Mater. 370, 130631. https://doi.org/10.1016/j.conbuildmat.2023.130631.

Fuertes, V., Reinosa, J.J., Fernández, J.F., Enríquez, E., 2022. Engineered feldspar-based ceramics: a review of their potential in ceramic industry. J. Eur. Ceram. Soc. 42 (2), 307–326. https://doi.org/10.1016/j.jeurceramsoc.2021.10.017.

Georgali, B., Tsakiridis, P.E., 2005. Microstructure of fire-damaged concrete. Case Stud. Cem. Concr. Compos. 27 (2), 255–259. https://doi.org/10.1016/j.cemconcomp.2004.02.022.

George, Skouteris, Ouki, Sabèha, Foo, Dominic, Saroj, Devendra, Altini, Maria, Melidis, Paraschos, Cowley, Brian, Ells, Geoff, Palmer, Stephanie, O'Dell, Sean, 2018. Water footprint and water pinch analysis techniques for sustainable water management in the brick-manufacturing industry. J. Clean. Prod. 172, 786–794. https://doi.org/10.1016/j.jclepro.2017.10.213.

Ghisellini, P., Ji, X., Liu, G., Ulgiati, S., 2018. Evaluating the transition towards cleaner production in the construction and demolition sector of China: a review. J. Clean. Prod. 195, 418–434. https://doi.org/10.1016/j.jclepro.2018.05.084.

Goel, Gaurav, Vasić, Milica Vidak, Kumar Katiyar, Nirmal, Kirthika, S.K., Pezo, Milada, Dinakar, P., 2021. Potential pathway for recycling of the paper mill sludge compost for brick making. Constr. Build. Mater. 278, 122384. https://doi.org/10.1016/j.conbuildmat.2021.122384.

González, I., Galán, E., Miras, A., Vázquez, M.A., 2011. CO2 emissions derived from raw materials used in brick factories. Applications to Andalusia (Southern Spain). Appl. Clay Sci. 52 (3), 193–198. https://doi.org/10.1016/j.clay.2011.01.003.

Hiroshima, Y., Hamamoto, Y., Yoshida, S., Matsuoka, J., 2008. Thermal conductivity of mixed alkali silicate glasses at low temperature. J. Non-Cryst. Solids 354 (2–9), 341–344. https://doi.org/10.1016/j.jnoncrysol.2007.08.082.

Kaya, S., Mançuhan, E., 2009. Küçükada, k, Modelling and optimization of the firing zone of a tunnel kiln to predict the optimal feed locations and mass fluxes of the fuel and secondary air. Appl. Energy 86 (3), 325–332. https://doi.org/10.1016/j.apenergy.2008.04.018.

Ke, S., Cheng, X., Wang, Y., Wang, Q., Wang, H., 2013. Dolomite, wollastonite and calcite as different CaO sources in anorthite-based porcelain. Ceram. Int. 39 (5), 4953–4960. https://doi.org/10.1016/j.ceramint.2012.11.091.

Klimesch, D.S., Ray, A., 1999. DTA-TGA evaluations of the CaO–Al2O3–SiO2–H2O system treated hydrothermally. Thermochim. Acta 334 (1–2), 115–122. https://doi.org/10.1016/S0040-6031(99)00140-9.

Koroneos, C., Dompros, A., 2007. Environmental assessment of brick production in Greece. Build. Environ. 42 (5), 2114–2123. https://doi.org/10.1016/j.buildenv.2006.03.006.

Kulkarni, N.G., Rao, A.B., 2016. Carbon footprint of solid clay bricks fired in clamps of India. J. Clean. Prod. 135, 1396–1406. https://doi.org/10.1016/j.jclepro.2016.06.152.

Leitner, J., Chuchvalec, P., Sedmidubský, D., Strejc, A., Abrman, P., 2002. Estimation of heat capacities of solid mixed oxides. Thermochim. Acta 395 (1–2), 27–46. https://doi.org/10.1016/S0040-6031(02)00177-6.

Lim, Seungmin, Mondal, Paramita, 2014. Micro- and nano-scale characterization to study the thermal degradation of cement-based materials. Mater. Char. 92, 15–25. https://doi.org/10.1016/j.matchar.2014.02.010.

Liu, Z., Meng, W., 2021. Fundamental understanding of carbonation curing and durability of carbonation-cured cement-based composites: a review. J. CO2 Util. 44, 101428. https://doi.org/10.1016/j.jcou.2020.101428.

Liu, M., Guo, J., Shao, Y., 2020. Effects of CaO and MgO contents on the properties of lightweight aggregate produced from municipal solid wastes. Constr. Build. Mater. 259, 120398. https://doi.org/10.1016/j.conbuildmat.2020.120398.

Liu, X., Feng, P., Cai, Y., Yu, X., Yu, C., Ran, Q., 2022. Carbonation behavior of calcium silicate hydrate (C-S-H): its potential for CO2 capture. Chem. Eng. J. 431 (3), 134243. https://doi.org/10.1016/j.cej.2021.134243.

Loryuenyong, V., Panyachai, T., Kaewsimork, K., Siritai, C., 2009. Effects of recycled glass substitution on the physical and mechanical properties of clay bricks. Waste Manag. 29 (10), 2717–2721. https://doi.org/10.1016/j.wasman.2009.05.015.

Lu, B., Shi, C., Zhang, J., Wang, J., 2018. Effects of carbonated hardened cement paste powder on hydration and microstructure of Portland cement. Constr. Build. Mater. 186, 699–708. https://doi.org/10.1016/j.conbuildmat.2018.07.159.

Ma, Z., Shen, J., Wu, H., Zhang, P., 2022. Properties and activation modification of eco-friendly cementitious materials incorporating high-volume hydrated cement powder from construction waste. Constr. Build. Mater. 316, 125788. https://doi.org/10.1016/j.conbuildmat.2021.125788.

Mahan, E.J., Hussein, A.K., 2017. Effect of additive type and percent on soil plasticity. Saudi J. Eng. Technol. 2 (2), 465–471. https://doi.org/10.21276/sjeat.2017.2.12.2.

Martínez-Martínez, S., Pérez-Villarejo, L., Garzón, E., Sánchez-Soto, P.J., 2023. Influence of firing temperature on the ceramic properties of illite-chlorite-calcitic clays. Ceram. Int. 49 (14-B), 24541–24557. https://doi.org/10.1016/j.ceramint.2022.11.077.

Martins Vaz, Igor Catão, Ghisi, Enedir, Piccinini Scolaro, Taylana, Schaefer, Aline, 2025. Understanding the environmental impacts of residential water consumption in Brazil: integrating the building stock with life cycle assessment. Build. Environ. 279, 113085. https://doi.org/10.1016/j.buildenv.2025.113085.

Mehdizade, H., Ling, T.-C., Cheng, X., Pan, S.-Y., Mo, K.H., 2021. CO2 treatment of hydrated cement powder: characterization and application consideration. J. Mater. Civ. Eng. 33 (4), 04021041. https://doi.org/10.1061/(ASCE)MT.1943-5533.0003652.

Morales, M.P., Juárez, M.C., Muñoz, P., Mendívil, M.A., Ruiz, J.A., 2014. Possibilities for improving the equivalent thermal transmittance of single-leaf walls for buildings. Energy Build. 69, 473–480. https://doi.org/10.1016/j.enbuild.2013.11.038.

Muñoz, P., Morales, M.P., Letelier, V., Mendívil, M.A., 2016. Fired clay bricks made by adding wastes: assessment of the impact on physical, mechanical and thermal properties. Constr. Build. Mater. 125, 241–252. https://doi.org/10.1016/j.conbuildmat.2016.08.024.

Muñoz, P., Letelier, V., Bustamante, M.A., Marcos-Ortega, J., Sepúlveda, J.G., 2020. Assessment of mechanical, thermal, mineral and physical properties of fired clay brick made by mixing kaolinitic red clay and paper pulp residues. Appl. Clay Sci. 198, 105847. https://doi.org/10.1016/j.clay.2020.105847.

Muñoz, P., Letelier, V., Muñoz, L., Bustamante, M.A., Gencel, O., Sutcu, M., 2021. The combined effect of bottom ashes and cellulose fibers on fired clay bricks. Constr. Build. Mater. 301, 124307. https://doi.org/10.1016/j.conbuildmat.2021.124307.

Muñoz, P., González, C., Recio, R., Gencel, O., 2022. The role of specific heat capacity on building energy performance and thermal discomfort. Case Stud. Constr. Mater. 17, e01423. https://doi.org/10.1016/j.cscm.2022.e01423.

Naumann, Gabriel, Schropp, Elke, Gaderer, Matthias, 2024. Environmental, economic, and eco-efficiency assessment of residential heating systems for low-rise buildings. J. Build. Eng. 98, 111074. https://doi.org/10.1016/j.jobe.2024.111074.

Ngun, B.K., Mohamad, H., Sulaiman, S.K., Okada, K., Ahmad, Z.A., 2011. Some ceramic properties of clays from central Cambodia. Appl. Clay Sci. 53 (1), 33–41. https://doi.org/10.1016/j.clay.2011.04.017.

Nigay, P.M., Cutard, T., Nzihou, A., 2017. The impact of heat treatment on the microstructure of a clay ceramic and its thermal and mechanical properties. Ceram. Int. 43 (2), 1747–1754. https://doi.org/10.1016/j.ceramint.2016.10.084.

Ohemeng, Eric A., 2023. Abdolhossein Naghizadeh, Alternative cleaner production of masonry mortar from fly ash and waste concrete powder. Constr. Build. Mater. 374, 130859. https://doi.org/10.1016/j.conbuildmat.2023.130859.

Osman, Gencel, Erdugmus, Ertugrul, Sutcu, Mucahit, Oren, Osman Hulusi, 2020. Effects of concrete waste on characteristics of structural fired clay bricks. Constr. Build. Mater. 255, 119362. https://doi.org/10.1016/j.conbuildmat.2020.119362.

Oubaha, Said, Taha, Yassine, Loutou, Mohamed, Mghazli, Mohamed Oualid, Benzaazoua, Mostafa, Hakkou, Rachid, 2023. Fired brick production using phosphogypsum and phosphate mining waste. Constr. Build. Mater. 403, 133149. https://doi.org/10.1016/j.conbuildmat.2023.133149.

Pardo, F., Jordan, M.M., Montero, M.A., 2018. Ceramic behaviour of clays in Central Chile. Appl. Clay Sci. 157, 158–164.

Phung, Q.T., Maes, N., Seetharam, S., 2019. Pitfalls in the use and interpretation of TGA and MIP techniques for Ca-leached cementitious materials. Mater. Des. 182, 108041. https://doi.org/10.1016/j.matdes.2019.108041.

Qiu, L., White, M.A., 2001. The constituent additivity method to estimate heat capacities of complex inorganic solids. J. Chem. Educ. 78 (8), 1076–1079. https://doi.org/10.1021/ed078p1076.

Rafael dos Santos, Macedo, Uliana, Daniel, Angulo, Sérgio Cirelli, Ulsen, Carina, 2024. Multistep chemical-mineralogical characterization to differentiate cement paste from carbonate rocks in CDW recycled aggregates. Constr. Build. Mater. 457, 139397. https://doi.org/10.1016/j.conbuildmat.2024.139397.

Real, S., Carriço, A., Bogas, J.A., Guedes, M., 2020. Influence of the treatment temperature on the microstructure and hydration behavior of thermoactivated recycled cement. Materials 13 (3937). https://doi.org/10.3390/ma13183937.

Sadik, C., El Amrani, I.-E., Albizane, A., 2014. Processing and characterization of alumina–mullite ceramics. J. Asian Ceram. Soc. 2 (4), 310–316. https://doi.org/10.1016/j.jascer.2014.07.006.

Semiz, B., 2017. Characteristics of clay-rich raw materials for ceramic applications in Denizli region (Western Anatolia). Appl. Clay Sci. 137, 83–93. https://doi.org/10.1016/j.clay.2016.12.014.

Silva, R.V., de Brito, J., Dhir, R.K., 2014. Properties and composition of recycled aggregates from construction and demolition waste suitable for concrete production. Constr. Build. Mater. 65, 201–217. https://doi.org/10.1016/j.conbuildmat.2014.04.117.

Slížková, Z., Gruber, M., Kostkanová, V., Frankeová, D., Wimmer-Frey, I., Drdácký, M., 2016. Soils and earthen building materials used for the buddhist temple complex. Int. J. Architect. Herit. 10 (4), 406–417. https://doi.org/10.1080/15583058.2014.991460.

Sousa, V., Bogas, J.A., 2021. Comparison of energy consumption and carbon emissions from clinker and recycled cement production. J. Clean. Prod. 306, 127277. https://doi.org/10.1016/j.jclepro.2021.127277.

Stebbins, J.F., Carmichael, I.S.E., Moret, L.K., 1984. Heat capacities and entropies of silicate liquids and glasses. Contrib. Mineral. Petrol. 86 (2), 131–148. https://doi.org/10.1007/BF00381840.

Tabit, K., Hajjou, H., Waqif, M., Saâdi, L., 2020. Effect of CaO/SiO2 ratio on phase transformation and properties of anorthite-based ceramics from coal fly ash and steel slag. Ceram. Int. 46 (6), 7550–7558. https://doi.org/10.1016/j.ceramint.2019.11.254.

Tang, Q., Ma, Z., Wu, H., Wang, W., 2020. The utilization of eco-friendly recycled powder from concrete and brick waste in new concrete: a critical review. Cement Concr. Compos. 114, 103807. https://doi.org/10.1016/j.cemconcomp.2020.103807.

Tavares-Brasileiro, C., Conte, S., Contartesi, F., Gomes-Melchiades, F., Zanelli, C., Dondi, M., Ortega-Boschi, A., 2021. Effect of strong mineral fluxes on sintering of porcelain stoneware tiles. J. Eur. Ceram. Soc. 41 (11), 5755–5767. https://doi.org/10.1016/j.jeurceramsoc.2021.04.027.

Tefa, Luca, Bianco, Isabella, Bassani, Marco, 2025. Stabilising CDW recycled aggregates with alternatives to Portland cement. Constr. Build. Mater. 471, 140705. https://doi.org/10.1016/j.conbuildmat.2025.140705.

Tokareva, Anna, Kaassamani, Sinan, Waldmann, Danièle, 2023a. Fine demolition wastes as Supplementary cementitious materials for CO2 reduced cement production. Constr. Build. Mater. 392, 131991. https://doi.org/10.1016/j.conbuildmat.2023.131991.

Tokareva, Anna, Kaassamani, Sinan, Waldmann, Danièle, 2023b. Fine demolition wastes as Supplementary cementitious materials for CO2 reduced cement production. Constr. Build. Mater. 392, 131991. https://doi.org/10.1016/j.conbuildmat.2023.131991.

Wang, J., Mu, M., Liu, Y., 2018. Recycled cement. Constr. Build. Mater. 190, 1124–1132. https://doi.org/10.1016/j.conbuildmat.2018.09.181.

Wang, Q., Zhang, J., Liu, J., Wu, W., Qi, W., Deng, H., 2020. Thermal conduction mechanism based on microstructural transformations of molten slag: the role of calcium oxide. Int. J. Heat Mass Tran. 160, 120167. https://doi.org/10.1016/j.ijheatmasstransfer.2020.120167.

Wang, S., Gainey, L., Baxter, D., Wang, X., Mackinnon, I.D.R., Xi, Y., 2021. Thermal behaviours of clay mixtures during brick firing: a combined study of in-situ XRD, TGA and thermal dilatometry. Constr. Build. Mater. 299, 124319. https://doi.org/10.1016/j.conbuildmat.2021.124319.

Wang, Haoyu, Xiong, Rui, Zong, Youjie, Li, Liding, Guo, Haoyan, Wang, Zhenjun, Guan, Bowen, Chang, Mingfeng, 2023. Effect of raw material ratio and sintering temperature on properties of coal gangue-feldspar powder artificial aggregate. Constr. Build. Mater. 384, 131400. https://doi.org/10.1016/j.conbuildmat.2023.131400.

Warrier, Ganga A., Palaniappan, Sivakumar, Habert, Guillaume, 2024. Classification of sources of uncertainty in building LCA. Energy Build. 305, 113892. https://doi.org/10.1016/j.enbuild.2024.113892.

Wei, W., Shao, Z., Qiao, R., Chen, W., Zhang, P., Cheng, J., 2021. Workability and mechanical properties of microwave heating for recovering high-quality aggregate from concrete. Constr. Build. Mater. 276, 122237. https://doi.org/10.1016/j.conbuildmat.2020.122237.

Wu, H., Zuo, J., Zillante, G., Wang, J., Yuan, H., 2019. Status quo and future directions of construction and demolition waste research: a critical review. J. Clean. Prod. 240, 118163. https://doi.org/10.1016/j.jclepro.2019.118163.

Xiao, J., Ma, Z., Sui, T., Akbarnezhad, A., Duan, Z., 2018. Mechanical properties of concrete mixed with recycled powder produced from construction and demolition waste. J. Clean. Prod. 188, 720–731. https://doi.org/10.1016/j.jclepro.2018.03.277.

Xiao, Jianzhuang, Shen, Jianyu, Bai, Meiyan, Qi, Gao, Wu, Yuching, 2021. Reuse of construction spoil in China: current status and future opportunities. J. Clean. Prod. 290, 125742. https://doi.org/10.1016/j.jclepro.2020.125742.

Yaras, A., Sutcu, M., Gencel, O., Erdogmus, E., 2019. Use of carbonation sludge in clay based building materials processing for eco-friendly, lightweight and thermal insulation. Constr. Build. Mater. 224, 57–65. https://doi.org/10.1016/j.conbuildmat.2019.07.080.

Zaid, S.N.A., Abdul Halim, M.S., Abdullah, M.A.A., Muhamad Nor, M.A.A., 2017. The effect of flux to physical and chemical properties of ceramic body using ball clay from kampung Dengir, Besut, Terengganu. Mater. Sci. Forum 888, 157–161. https://doi.org/10.4028/www.scientific.net/msf.888.157.

Zat, Tuani, Bandieira, Mariana, Sattler, Naquiele, Segadães, Ana M., Cruz, Robinson C.D., Mohamad, Gihad, Rodríguez, Erich D., 2021. Potential re-use of sewage sludge as a raw material in the production of eco-friendly bricks. J. Environ. Manag. 297, 113238. https://doi.org/10.1016/j.jenvman.2021.113238.

Zhao, Jianhua, Feng, Shuo, Grunewald, John, Meissner, Frank, Wang, Jiehui, 2022. Drying characteristics of two capillary porous building materials: calcium silicate and ceramic brick. Build. Environ. 216, 109006. https://doi.org/10.1016/j.buildenv.2022.109006.

Zhong, Li, Bian, Yadong, Zhao, Jihui, Wang, Yiren, Yuan, Zhenxia, 2022. Recycled concrete fine powder (RFP) as cement partial replacement: influences on the physical properties, hydration characteristics, and microstructure of blended cement. J. Build. Eng. 62, 105326. https://doi.org/10.1016/j.jobe.2022.105326.

Zhou, X., Liu, D., Bu, H., Deng, L., Liu, H., Yuan, P., Du, P., Song, H., 2018. XRD-based quantitative analysis of clay minerals using reference intensity ratios, mineral intensity factors, Rietveld, and full pattern summation methods: a critical review. Solid Earth Sci. 3 (1), 16–29. https://doi.org/10.1016/j.sesci.2017.12.002.

Zhu, D., Wang, D., Pan, J., Guo, Z., Yang, C., 2022. Utilization of hydrated lime as binder and fluxing agent for the production of high basicity magnesium fluxed pellets. ISIJ Int. 62 (4), 632–641. https://doi.org/10.2355/isijinternational.ISIJINT-2021-157.